CHINESE JOURNAL OF PHYSICS

ISSN: 0577-9073; IMPACT FACTOR= 0514
PUBLISHER: ELSEVIER

Accepted August 7th 2017

BIOCONVECTION NANOFLUID SLIP FLOW PAST A WAVY SURFACE WITH APPLICATIONS IN NANO-BIOFUEL CELLS

M.J. Uddin*[1], W.A. Khan[2], **S**.R. Qureshi[3] and O. Anwar Bég[4]

[1]*Mathematics Department, American International University-Bangladesh, Banani,Dhaka 1213,* ***Bangladesh, Email:*** ***jashim_74@yahoo.com***

[2] *Department of Mechanical and Industrial Engineering College of Engineering, Majmaah University,* ***Saudia Arabia, Email:*** ***wkhan_20002@yahoo.com***

[3]*Department of Engineering Sciences, PN Engineering College, National University of Sciences and Technology, Karachi 75350,* ***Pakistan, Email:*** ***shafiqpn1@gmail.com***

[4]*Aeronautical and Mechanical Engineering, Room G77, Newton Building, School of Computing, Science and Engineering (CSE), University of Salford, M54WT,* ***UK, Email:*** ***O.A.Beg@salford.ac.uk***

Abstract

A theoretical study is presented to examine free convective boundary layer flow of water-based bio-nanofluid containing gyrotactic microorganisms past a wavy surface. Buongiorno's nanofluid model with passively controlled boundary condition is applied to investigate the effects of the emerging parameters on the physical quantities namely, skin friction, Nusselt numbers and density number of motile microorganisms. The effects of the both hydrodynamic and thermal slips are also incorporated. Local similarity and non-similarity solutions are obtained using the seventh-order Runge-Kutta-Fehlberg method (RKF7) coupled with shooting quadrature. In order to compare our numerical results with the existing data, the active mass flux boundary condition is also used to benchmark MAPLE numerical solutions with earlier similar and non-similar solutions for a smooth stationary surface. It is found that the passive boundary condition reduces the skin friction and enhances local Nusselt numbers. Also the wavy surface is found to result in higher skin friction and higher local Nusselt numbers compared with a stationary surface. It is found that motile micro-organism density number is elevated with increasing bioconvection Péclet number whereas the motile micro-organism species boundary layer thickness is reduced with increasing bioconvection Lewis number. The work finds applications in heat transfer enhancement in bio-inspired nanoparticle-doped fuel cells.

Keywords: Bioconvection; passively controlled horizontal wavy surface; multiple slip effects; non-similar, biofuel cells.

***Corresponding author: Email: jashim_74@yahoo.com**

1. Introduction

Nanofluid applications in medical engineering are stimulating significant attention. Areas being explored range from pharmacodynamics [1] to plant-inspired biofuel cells [2]. Applications in bio-

energy systems and in particular proton exchange membrane (PEM) bio-inspired fuel cells are also increasing [3]. Nanofluids offer a significant thermal enhancement characteristic as compared to tradition fluids. They also enable manipulation of designs at the nanoscale, which is of great interest in bio-nano-technology. An alternative methodology for enhancing heat/mass/microorganism transfer is geometric modification of the surfaces adjacent to the transport medium i.e. biofluid. Examples of this geometric modification include *irregular or wavy surfaces* which have been successfully used in a wide spectrum of technological applications including microbial fuel cell walls [4,5], plant engineering-inspired bio fuel production [6,7] and solar collectors. The wavy surface may be vertical/inclined or horizontal depending upon its application. In the context of biofuel cell design, a lot of new developments in the structure of wall surfaces and polymers have enabled engineers to explore wavy heat transfer as a viable improved system which can significantly enhance fuel efficiencies achievable [7]. Free and mixed convective flow past a wavy surfaces have been studied by many scientist. Representative studies in this area include [8]-[15]. These largely theoretical and computational studies have used for many hydrodynamic, thermal, concentration and microorganism boundary conditions. They found that the frequency of the local heat transfer rate is double that of the wavy surface. In the studies [8-15] many multi-physical effects such as the temperature-dependent viscosity, heat generation/absorption, buoyancy ratio, magnetic parameter, the amplitude of the wavy surface and Prandtl number on the skin friction, dimensionless rate of heat and mass transfer were investigated. Natural or mixed convection heat and mass transfer from inclined wavy surfaces in porous media saturated with different fluids has also been investigated by a number of researchers. Cheng [16] studied the double diffusive free convective flow near an inclined wavy surface in porous medium with constant wall temperature and concentration and found that a decrease in the angle of inclination lead to increase fluctuation of the local Nusselt and Sherwood numbers, and further noting that increasing the angle of inclination tends to increase the total heat and mass transfer rates. In another study, Cheng [17] also solved the problem of free convection boundary layer flow near an inclined wavy surface. Abdallah and Zeghmati [18] studied numerical effects of wavy surfaces and thermal radiation on free convective heat transfer along an inclined wavy plate. D'Alessio *et al.* [19] discussed the two-dimensional problem of gravity-driven laminar flow of a thin layer of fluid down a heated wavy inclined surface. They conducted a stability analysis and used nonlinear simulations to validate the stability predictions and also to study thermo-capillary effects. The effects of thermal stratification and radiation on nanofluid flow past an inclined wavy surface embedded in a non-Darcy porous medium were studied by Srinivasacharya and Kumar [20].

Horizontal wavy surfaces geometries have been used by many investigators. Siddiqa and Hossain [21] analyzed convective flow. Siddiqa *et al.* [22] illustrated free convective flow past radiative wavy surface. They reported that wavy surface enhances heat transfer rate compared to the smooth wall and that high amplitude of the wavy surface leads to separation of fluid from the plate. In another report, Siddiqa *et al.* [23] examined the natural convective flow from an irregular semi-infinite triangular wavy surface, obtaining solutions for the skin friction, heat transfer rate, streamlines and isotherm distributions. Rees and Pop [24] studied the effect of stationary surface waves on the natural convective flow induced due to a horizontal plate in a porous medium. They performed extensive computations for a wide range of wave amplitudes and phases and found that a thin near-wall boundary layer develops within the basic boundary layer as the distance downstream increases. Narayana *et al.* [25] discussed the double diffusive convection induced by a heated and salted horizontal wavy surface. Hossain and Pop [26] reported flow and heat transfer on a continuous moving wavy surface in a stationary fluid with magnetic field. Tashtoush and Abu-Irshaid [27] investigated heat transfer along a wavy surface with a prescribed heat flux. They found that for a given amplitude, a point of separation appears rendering the solution restricted at that amplitude. Murrhy *et al.* [28] analyzed the effect of surface undulations on the natural convection heat transfer from an isothermal surface in a Darcian fluid-saturated porous enclosure, indicating that the wavy wall reduces the heat transfer into the system. Reddy *et al*. [29] investigated the flow and heat transfer past a continuous moving surface in a Darcian porous medium. The free convective flow along horizontal and slightly inclined surfaces was studied by Pera and Gebhart [30]. They measured the temperature distributions and heat transfer parameters in air at atmospheric pressure. Pradhan *et al*. [31] considered the natural convective flow of a water-based nanofluid along an isothermal horizontal plate.

Nanofluids can change the transport as well as thermal properties of the carrier fluid and consequently enhance thermal as well mass and microorganism transport. These fluids are engineered colloids comprising a base fluid (e.g. water) and nanoparticles (e.g. metallic or non-metalic particles). When microorganisms which are heavier than water are present with nanoparticles in water, bioconvection occur due to the movement of microorganisms in a specific direction [32-33]. Kuznetsov and Avramenko [34] and Kuznetsov and Geng [35-38] investigated theoretically the bioconvection behavior of suspensions of gyrotactic microorganisms. The concept of *nanofluid bioconvection* was probably first introduced by Kuznetsov [39-40]. Kuznetsov [41] further developed this theory and focused on nanofluids containing gyrotactic microorganisms, confirming that the resultant large-scale motion of fluid caused by self-propelled motile microorganisms enhances mixing and prevents nanoparticle agglomeration in nanofluids. Aziz *et al.* [42] applied Buongiorno's model [43] to study boundary layer flow of nanofluid with gyrotactic microorganism.

Kuznetsov and Nield [44-45] revisited the problems of natural convective flow of a nanofluid and extended their models to the case when the nanofluid particle fraction on the boundary is *passively* rather than *actively* controlled. This makes the model physically more realistic than the previous models and more relevant to actual engineering systems. Subsequently Khan *et al.* [46] employed the same boundary condition which accounts for the effect of both Brownian and thermophoresis parameters. According to this new type of boundary condition there exists zero nanoparticle flux at the surface and the particle fraction values adjust accordingly. A book on wavy surface has been produced recently by Shenoy et al. [47]. Sadia et al. [48] studied gyrotactic bioconvection flow of a nanofluid past a vertical wavy surface. Naheed et al. [49] studied nanofluid bioconvection with variable thermophysical properties. Sheikholeslami and Rokni [50] studied the effect of melting heat transfer on nanofluid flow in the presence of a magnetic field using the Buongiorno model. Soomro et al. [51] investigated the effect of passive control boundary on nanoparticle due to convective heat transfer of Prandtl fluid model for the stretching surface.

The above review of literature reveals that there is no study of free convective flow of water-based nanofluids with microorganism along a horizontal wavy surface with passively controlled boundary condition. This has motivated the present investigation and is particularly relevant to microbial fuel cells exploiting both nanofluids and bioconvection. Local similarity and non-similarity solutions of the transport equations are obtained by using the Runge-Kutta-Fehlberg method of seventh order (RKF7) coupled with a shooting method. The effects of the emerging parameters on the dimensionless velocity, temperature, nanoparticle volume fraction, and motile microorganism along with the skin friction, the rate of heat transfer and the rate of motile microorganism transfer are examined numerically and discussed in details. The numerical results are found to demonstrate good agreement with the published results for certain special cases. The present work is aimed at further elucidating the near-wall transport phenomena encountered in bio-nanofluid fuel cells [2-7].

2. Formulation of the Problem

We consider the steady flow of a water-based nanofluid along a stationary/moving horizontal wavy surface in a clam free stream. It is assumed that the nanofluid contains gyrotactic microorganisms. It is also assumed that the nanoparticle suspension is stable and the direction of microorganisms' swimming is independent of nanoparticles. The fluid is considered to be homogeneous and incompressible, and the volume fraction of the micro-organisms is sufficiently small such that they exert a negligible effect on the inertia and the viscosity of the fluid–microbe suspension. The flow model and coordinate system is depicted in **Fig.1**. The temperature T_w and the density of motile microorganisms n_w are assumed at the

surface, whereas, T_∞, C_∞ and n_∞ are assumed as surrounding temperature, concentration and density of motile microorganisms. We used the *passively controlled* (PC) boundary condition which is imposed at the surface (Kuznetsov and Nield [44, 45]). Considering the Oberbeck-Boussinesq approximation and following Buongiorno [42], Kuznetsov and Nield [39], the continuity and momentum equations are:

$$\frac{\partial \bar{u}}{\partial \bar{x}} + \frac{\partial \bar{v}}{\partial \bar{y}} = 0, \tag{1}$$

$$\rho_f \left(\bar{u} \frac{\partial \bar{u}}{\partial \bar{x}} + \bar{v} \frac{\partial \bar{u}}{\partial \bar{y}} \right) = -\frac{\partial \bar{p}}{\partial \bar{x}} + \frac{\nu}{\rho_f} \frac{\partial^2 \bar{u}}{\partial \bar{y}^2}, \tag{2}$$

$$-\frac{\partial \bar{p}}{\partial \bar{y}} + \left[(1 - C_\infty) \rho_f \, g \, \beta (T - T_\infty) - (\rho_{\bar{p}} - \rho_f) g (C - C_\infty) \right] + \gamma (\rho_{\bar{p}} - \rho_f) g \, n = 0. \tag{3}$$

The thermal energy equation:

$$\bar{u} \frac{\partial T}{\partial \bar{x}} + \bar{v} \frac{\partial T}{\partial \bar{y}} = \alpha \frac{\partial^2 T}{\partial \bar{y}^2} + \tau \left[D_B \frac{\partial C}{\partial \bar{y}} \frac{\partial T}{\partial \bar{y}} + \left(\frac{D_T}{T_\infty} \right) \left(\frac{\partial T}{\partial \bar{y}} \right)^2 \right]. \tag{4}$$

The conservation of the nanoparticles:

$$\bar{u} \frac{\partial C}{\partial \bar{x}} + \bar{v} \frac{\partial C}{\partial \bar{y}} = D_B \frac{\partial^2 C}{\partial \bar{y}^2} + \left(\frac{D_T}{T_\infty} \right) \frac{\partial^2 T}{\partial \bar{y}^2}. \tag{5}$$

The conservation of micro-organisms equation

$$\bar{u} \frac{\partial n}{\partial \bar{x}} + \bar{v} \frac{\partial n}{\partial \bar{y}} + \frac{\partial}{\partial \bar{y}} (n \tilde{v}) = D_n \frac{\partial^2 n}{\partial \bar{y}^2}. \tag{6}$$

The left-hand side of Eq. (6) represents the flux of microorganisms due to the macroscopic motion of the fluid, the directional swimming of microorganisms up the oxygen gradients, and a diffusive process that models all random motions of the microorganisms. Here α is the thermal diffusivity, $\tau = \frac{(\rho c)_{\bar{p}}}{(\rho c)_f}$ is the ratio of the effective heat capacity of the nanoparticle and fluid, ρ_f is the density of the fluid, μ is the dynamic viscosity, β is the volumetric expansion of fluid, $\rho_{\bar{p}}$ is the density of the nanoparticles, $\bar{\gamma}$ is the average volume of the micro-organism, $(\rho c)_f$ is the heat effective heat capacity of the fluid, $(\rho c)_{\bar{p}}$ is the effective heat capacity of the nanoparticle material, k is the effective thermal conductivity, g is the gravitation due to acceleration, D_B is the Brownian diffusion coefficient, D_T is the thermophoretic diffusion coefficient, $(\bar{u}, \bar{v})$ are the velocity components along the axes,

$U_r = \dfrac{\alpha}{L} Ra^{2/5}$ is the reference velocity, L is the reference length, $\bar{u}_{\text{slip}} = \dfrac{\mu}{\rho} N_1 \dfrac{\partial \bar{u}}{\partial \bar{y}}$ is the linear slip velocity, N_1 is the velocity slip factor, $T_{\text{slip}} = D_1 \dfrac{\partial T}{\partial \bar{y}}$ is the thermal slip, D_1 is the thermal slip factor, $\bar{\alpha}$ is the dimensional amplitude of wavy surface, ω is the phase sift parameter, $\tilde{v} = \left(\dfrac{bW_c}{\Delta C_\infty} \right) \dfrac{\partial C}{\partial \bar{y}}$, D_n is the diffusivity of microorganisms, b is the chemotaxis constant [m] and W_c is the maximum cell swimming speed [m/s] (the product bW_c is assumed to be constant. It is assumed that sheet velocity is $N_1(\bar{x}/L) = (N_1)_0 \left(\dfrac{\bar{x}}{L} \right)^{2/5}$, $D_1(\bar{x}/L) = (D_1)_0 \left(\dfrac{\bar{x}}{L} \right)^{2/5}$. Here $\lambda = 0$ stands for a stationary plate, $\lambda = 1$ is associated with the case of a moving plate.

The geometry of the wavy surface is described by:

$$\bar{y} = \bar{\alpha} \sin(\pi \bar{x}/L - \omega). \tag{7}$$

where $\bar{\alpha}$ is the amplitude, ω is the phase shift parameter and L is the characteristic length as shown in Fig. 1. The physically realistic boundary conditions are (Karniadakis *et al.* [52]):

$$\begin{aligned} &\bar{u} = \lambda \bar{u}_w(\bar{x}/L) + \bar{u}_{\text{slip}}, \ \bar{v} = 0, T = T_w(\bar{x}/L) + T_{\text{slip}}, \ \ n = n_w, \\ &\text{at } \bar{y} = \bar{\alpha} \sin(\pi \bar{x}/L - \omega), \forall \bar{x} \\ &\bar{u} \to 0, \ T \to T_\infty, \ C \to C_\infty, \ \bar{p} \to \bar{p}_\infty, n = 0 \text{ as } \bar{y} \to \infty, \forall \bar{x}. \end{aligned} \tag{8}$$

The *mass flux boundary condition* [44, 45] can be written as

$$\begin{aligned} &D_B \frac{\partial C}{\partial \bar{y}} + \frac{D_T}{T_\infty} \frac{\partial T}{\partial \bar{y}} = 0 \ \text{(passive control)} \\ &C = C_w \qquad \text{(active control)} \end{aligned} \tag{9}$$

It is pertinent to introduce a group of dimensionless variables to render Eqns. (1) - (6) into non-dimensional form. These are defined as follows:

$$\begin{aligned} &x = \frac{\bar{x}}{L}, \ y = \frac{\bar{y}}{L} Ra^{1/5}, \ \ u = \frac{L}{\alpha} Ra^{-2/5} \bar{u}, \ \ \text{v} = \frac{L}{\alpha} Ra^{-1/5} \bar{u}, \ \ \theta = \frac{T - T_\infty}{T_w - T_\infty}, \\ &\chi = \frac{n}{n_w}, \ \ p = \frac{L^2 (\bar{p} - \bar{p}_\infty)}{\rho_f \alpha^2} Ra^{-4/5}, \end{aligned} \tag{10}$$

$$\begin{aligned} &\phi = \frac{C - C_\infty}{C_w - C_\infty} \qquad \text{for actively control} \\ &\phi = \frac{C - C_\infty}{C_\infty} \qquad \text{for passively control} \end{aligned} \tag{11}$$

where $Ra = g\beta(1 - C_\infty)(T_w - T_\infty) L^3 \rho_f / (\alpha \mu)$ is the Rayleigh number. A stream function ψ defined by

$u = \dfrac{\partial \psi}{\partial y}$ and $v = -\dfrac{\partial \psi}{\partial x}$ is introduced into Eqns. (2) - (5) which satisfies Eq. (1) identically. Hence

$$\mathrm{Pr}\frac{\partial^3 \psi}{\partial y^3} - \frac{\partial p}{\partial x} + \frac{\partial \psi}{\partial x}\frac{\partial^2 \psi}{\partial y^2} - \frac{\partial \psi}{\partial y}\frac{\partial^2 \psi}{\partial y \partial x} = 0, \tag{12}$$

$$-\frac{1}{\mathrm{Pr}}\frac{\partial p}{\partial y} + \theta - Nr\,\phi + Rb\,\chi = 0, \tag{13}$$

$$\frac{\partial \psi}{\partial y}\frac{\partial \theta}{\partial x} - \frac{\partial \psi}{\partial x}\frac{\partial \theta}{\partial y} - \frac{\partial^2 \theta}{\partial y^2} - Nb\frac{\partial \theta}{\partial y}\frac{\partial \phi}{\partial y} - Nt\left(\frac{\partial \theta}{\partial y}\right)^2 = 0, \tag{14}$$

$$Le\left[\frac{\partial \psi}{\partial y}\frac{\partial \phi}{\partial x} - \frac{\partial \psi}{\partial x}\frac{\partial \phi}{\partial y}\right] - \frac{\partial^2 \phi}{\partial y^2} - \frac{Nt}{Nb}\frac{\partial^2 \theta}{\partial y^2} = 0, \tag{15}$$

$$Lb\left[\frac{\partial \psi}{\partial y}\frac{\partial \chi}{\partial x} - \frac{\partial \psi}{\partial x}\frac{\partial \chi}{\partial y}\right] - Pe\left[\chi\frac{\partial^2 \phi}{\partial y^2} + \frac{\partial \chi}{\partial y}\frac{\partial^2 \phi}{\partial y^2}\right] - \frac{\partial^2 \chi}{\partial y^2} = 0. \tag{16}$$

The boundary conditions in Eqn. (7) become:

$$\frac{\partial \psi}{\partial x} = 0,\ \frac{\partial \psi}{\partial y} = \lambda x^{1/5} + a\,x^{2/5}\frac{\partial^2 \psi}{\partial y^2},\ \theta = 1 + b\,x^{2/5}\frac{\partial \theta}{\partial y},\ Nb\,\phi' + Nt\,\theta' = 0,\ \chi = 1 \text{ at } y = \alpha_0 \sin(\pi x - \omega),$$
$$\frac{\partial \psi}{\partial y} \to 0,\ \theta \to 0,\ \phi \to 0,\ p \to 0, \chi \to 0 \text{ as } y \to \infty. \tag{17}$$

The mass flux boundary condition at $y = \alpha_0 \sin(\pi x - \omega)$ can be written as:

$$\begin{aligned} &Nb\,\phi' + Nt\,\theta' = 0 \quad \text{for passive control} \\ &\phi = 1 \quad\quad\quad\ \text{for active control} \end{aligned} \tag{18}$$

The dimensionless parameters in Eqns. (12) - (16) are defined as

$$\mathrm{Pr} = \frac{\nu}{\alpha} \text{ (Prandtl number)}, \tag{19}$$

$$Nr = \frac{\left(\rho_p - \rho_f\right)\left(C_w - C_\infty\right)}{\rho_f\,\beta\left(1 - C_\infty\right)\left(T_w - T_\infty\right)} \text{ (buoyancy ratio)}, \tag{20}$$

$$Rb = \frac{\gamma\left(\rho_p - \rho_f\right)n_w}{\rho_f\,\beta\left(1 - C_\infty\right)\left(T_w - T_\infty\right)} \text{ (bioconvection Rayleigh number)}, \tag{21}$$

$$Le = \frac{\alpha}{D_B} \text{ (Lewis number)}, \tag{22}$$

$$Nb = \frac{\tau D_B \left(C_w - C_\infty\right)}{\alpha} \text{ (Brownian motion parameter)}, \tag{23}$$

$$Nt = \frac{\tau D_T \left(T_w - T_\infty\right)}{\alpha T_\infty} \text{ (thermophoresis parameter)}, \tag{24}$$

$$Lb = \frac{\nu}{D_B} \text{ (bioconvection Lewis number)}, \tag{25}$$

$$Pe = \frac{\tilde{b} W_c}{D_n} \text{ (Peclet number)}, \tag{26}$$

$$a = \frac{N_1 \mu Ra^{1/5}}{\rho_f L} \text{ (velocity slip)}, \tag{27}$$

$$b = \frac{D_1 Ra^{1/5}}{L} \text{ (thermal slip)}, \tag{28}$$

$$\alpha_0 = \frac{\bar{\alpha}}{L} Ra^{1/5} \text{ (amplitude of the wavy surface)}. \tag{29}$$

Following Siddiqa *et al*. [22], we invoke the following transformations:

$$\begin{aligned} &\eta = \xi^{-\frac{2}{5}}\left[y - \alpha_0 \sin\left(\pi\xi - \omega\right)\right],\ \psi = \xi^{\frac{3}{5}} f(\xi,\eta),\ p = \xi^{\frac{2}{5}} h(\xi,\eta), \\ &\theta = \theta(\xi,\eta),\ \phi = \phi(\xi,\eta),\ \chi = \chi(\xi,\eta),\ \xi = x. \end{aligned} \tag{30}$$

On substituting the transformations specified in Eq. (15) into the governing Eqns. (12) - (16), we obtain the following similarity ordinary differential equations:

$$\Pr f''' + \frac{3}{5} f f'' - \frac{1}{5} f'^2 + \left[\frac{2}{5}\eta + \alpha_0 \pi \xi^{3/5} \cos\left(\pi\xi - \omega\right)\right] h' - \frac{2}{5} h = \xi\left(f' \frac{\partial f'}{\partial \xi} - f'' \frac{\partial f}{\partial \xi} + \frac{\partial h}{\partial \xi}\right), \tag{31}$$

$$-\frac{1}{\Pr} h' + \theta - Nr\ \phi + Rb\ \chi = 0, \tag{32}$$

$$\theta'' + \frac{3}{5}\ f\ \theta' + Nb\ \theta'\ \phi' + Nt\ \theta'^2\ = \xi\left(f' \frac{\partial \theta}{\partial \xi} - \theta' \frac{\partial f}{\partial \xi}\right), \tag{33}$$

$$\phi'' + \frac{3}{5} Le\ f\ \phi' + \frac{Nt}{Nb}\theta'' = Le\ \xi\left(f' \frac{\partial \phi}{\partial \xi} - \phi' \frac{\partial f}{\partial \xi}\right), \tag{34}$$

$$\chi'' - Pe\left[\chi'\phi' + \chi\phi''\right] + \frac{3}{5} Lb\ f\ \chi' = Lb\ \xi\left(f' \frac{\partial \chi}{\partial \xi} - \chi' \frac{\partial f}{\partial \xi}\right). \tag{35}$$

The transformed boundary conditions can be written as:

$$\begin{aligned} &f(\xi,0) = 0,\ f'(\xi,0) = \lambda + a\ f''(\xi,0),\ \theta(\xi,0) = 1 + b\theta'(\xi,0),\ Nb\ \phi'(\xi,0) + Nt\ \theta'(\xi,0) = 0, \\ &\chi(\xi,0) = 1,\ f'(\xi,\infty) = \theta(\xi,\infty) = \phi(\xi,\infty) = h(\xi,\infty) = 0,\ \chi(\xi,\infty) = 0, \end{aligned} \tag{36}$$

where primes denote differentiation with respect to η. It is important to note that when $\alpha_0 = 0$, Eq. (31) represents the scenario of a horizontal flat plate i.e. waviness is eliminated.

3 Physical Quantities

The local skin friction factor $C_{f\,\bar{x}}$, the local Nusselt number $Nu_{\bar{x}}$ and the local density number of motile microorganisms $Nn_{\bar{x}}$ are the parameters of engineering interest. These quantities can be obtained from the following relations:

$$C_{f\,\bar{x}} = \frac{2\mu}{\rho \bar{u}_w^2}\left(\frac{\partial \bar{u}}{\partial \bar{y}}\right)_{\bar{y}=0}, \quad Nu_{\bar{x}} = \frac{-\bar{x}}{T_w - T_\infty}\left(\frac{\partial T}{\partial \bar{y}}\right)_{\bar{y}=0}, Nn_{\bar{x}} = \frac{-\bar{x}}{n_w}\left(\frac{\partial n}{\partial \bar{y}}\right)_{\bar{y}=0} \tag{37}$$

Using Eqns. (7) and (15) into Eq. (21), the following expressions emerge:

$$Ra_{\bar{x}}^{3/5} C_{f\,\bar{x}} = f''(\xi,0),\ Ra_{\bar{x}}^{-1/5} Nu_{\bar{x}} = -\theta'(\xi,0), Ra_{\bar{x}}^{-1/5} Nn_{\bar{x}} = -\chi'(\xi,0) \tag{38}$$

Here $Ra_{\bar{x}} = g\beta(1-C_\infty)\Delta T\ \bar{x}^3/(\alpha\nu)$ is the local Rayleigh number. Due to zero mass flux boundary condition, local Sherwood number will be zero. Following [44, 45], the reduced skin friction, Nusselt number and density number of motile microorganisms can be written as

$$Cf_r = f''(\xi,0),\ Nur = -\theta'(\xi,0), Nn_r = -\chi'(\xi,0) \tag{39}$$

4. Numerical Solution of Boundary Value Problem

4.1 First Level of Truncation (Local *Similarity*)

Equations (31) - (35) with associated boundary conditions (36) constitute highly nonlinear ordinary differential boundary value problem. A numerical solution is therefore developed here. Following Sparrow *et al.* [53, 54], for the first level of truncation, it is assumed that the ξ-derivatives in Eqns. (31) - (35) are neglected and these equations can be rewritten as:

$$\Pr f''' + \frac{3}{5} f f'' - \frac{1}{5} f'^2 + \left[\frac{2}{5}\eta + \alpha_0 \pi \xi^{3/5}\cos(\pi\xi - \omega)\right] h' - \frac{2}{5} h = 0, \tag{40}$$

$$-\frac{1}{\Pr} h' + \theta - Nr\ \phi + Rb\ \chi = 0, \tag{41}$$

$$\theta'' + \frac{3}{5} f\ \theta' + Nb\ \theta'\ \phi' + Nt\ \theta'^2 = 0, \tag{42}$$

$$\phi'' + \frac{3}{5} Le\ f\ \phi' + \frac{Nt}{Nb}\theta'' = 0, \tag{43}$$

$$\chi'' - Pe\left[\chi'\phi' + \chi\phi''\right] + \frac{3}{5} Lb\ f\ \chi' = 0. \tag{44}$$

These equations along with boundary conditions (36) present a local similarity model where ξ can be regarded as a parameter. This model can be solved numerically using the Runge-Kutta-Fehlberg method of seventh order (RKF7) coupled with a shooting method [55]. The computations are shown in **Table 1** for the flow of nanofluids over a smooth horizontal surface (i.e. waviness is negated). We further note that more details of the numerical procedure employed are documented in Minkowycz

and Sparrow [55]. More recent applications of this method include dispersive and stratified porous media convection [56], liquid metal magneto-hydrodynamic induction heat transfer [57] and solar collector cross-diffusion transport phenomena [58].

4.2 Second Level of Truncation (Local *non-similarity*)

Following Sparrow and co-workers [53, 54], all the terms are retained in Eqns. (31) - (35) without any approximation and new auxiliary functions $F(\xi,\eta), \mathrm{H}(\xi,\eta), \Theta(\xi,\eta), \Phi(\xi,\eta), \Xi(\xi,\eta)$ are assumed which are defined by:

$$F=\frac{\partial f}{\partial \xi}, \mathrm{H}=\frac{\partial h}{\partial \xi}, \Theta=\frac{\partial \theta}{\partial \xi}, \Phi=\frac{\partial \phi}{\partial \xi}, \Xi=\frac{\partial \chi}{\partial \xi} \tag{45}$$

Using these functions, Eqns. (31) - (35) can be re-written as

$$\mathrm{Pr}\, f'''+\frac{3}{5} f\, f''-\frac{1}{5} f'^{2}+\left[\frac{2}{5}\eta+\alpha_0 \pi\, \xi^{3/5}\cos(\pi\xi-\omega)\right] h'-\frac{2}{5} h=\xi\left(f'F'-f''F+\mathrm{H}\right), \tag{46}$$

$$-\frac{1}{\mathrm{Pr}} h'+\theta-Nr\ \phi+Rb\,\chi=0, \tag{47}$$

$$\theta''+\frac{3}{5}\, f\ \theta'+Nb\ \theta'\ \phi'+Nt\ \theta'^{2}\ =\xi\left(f'\Theta-\theta' F\right), \tag{48}$$

$$\phi''+\frac{3}{5} Le\, f\, \phi'+\frac{Nt}{Nb}\theta''=Le\,\xi\left(f'\Phi-\phi' F\right), \tag{49}$$

$$\chi''-Pe\left[\chi'\phi'+\chi\phi''\right]+\frac{3}{5} Lb\, f\, \chi'=Lb\,\xi\left(f'\Xi-\chi' F\right). \tag{50}$$

Differentiating Eqns. (47) - (51) and boundary conditions (36) with respect to ξ and neglecting again ξ-derivatives, we get:

$$\begin{aligned}&\mathrm{Pr}\, F'''+\frac{3}{5} F\, f''+\frac{3}{5} fF''-\frac{2}{5} fF'+\left[\frac{3}{5}\alpha_0 \pi\, \xi^{-2/5}\cos\left(-\pi\xi+\omega\right)+\alpha_0 \pi^{2}\xi^{3/5}\sin\left(-\pi\xi+\omega\right)\right] h'+\\ &\left[\frac{2}{5}\eta+\alpha_0 \pi\, \xi^{3/5}\cos\left(-\pi\xi+\omega\right)\right]\mathrm{H}'-\frac{2}{5}\mathrm{H}'-\left(f'F'-f''F+\mathrm{H}\right)=0\end{aligned} \tag{51}$$

$$-\frac{1}{\mathrm{Pr}}\mathrm{H}'+\Theta-Nr\ \Phi+Rb\,\Xi=0, \tag{52}$$

$$\Theta''+\frac{3}{5}\left(F\ \theta'+f\Theta'\right)+Nb\left(\Theta'\ \phi'+\theta'\Phi'\right)+2Nt\ \theta'\Theta'-\left(f'\Theta-\theta' F\right)=0, \tag{53}$$

$$\Phi''+\frac{3}{5} Le\left(F\,\phi'+f\,\Phi'\right)+\frac{Nt}{Nb}\Theta''-Le\left(f'\Phi-\phi' F\right)=0, \tag{54}$$

$$\Xi''-Pe\left[\Xi'\phi'+\chi'\Phi'+\Xi\phi''+\chi\Phi''\right]+\frac{3}{5} Lb\left(F\,\chi'+f\,\Xi'\right)-Lb\left(f'\Xi-\chi' F\right). \tag{55}$$

The additional boundary conditions are:

$$F(\xi,0)=0,\ F'(\xi,0)=a\,F''(\xi,0),\ \Theta(\xi,0)=b\,\Theta'(\xi,0),\ Nb\,\Phi'(\xi,0)+Nt\,\Theta'(\xi,0)=0,$$
$$\Xi(\xi,0)=0,\ F'(\xi,\infty)=\Theta(\xi,\infty)=\Phi(\xi,\infty)=\mathrm{H}(\xi,\infty)=0,\ \Xi(\xi,\infty)=0, \tag{56}$$

Equations (52)-(55) with boundary conditions (56) represent a *local non-similarity model*. This model with Eqns. (47)-(51) with boundary conditions (36) can be solved numerically using the Runge-Kutta-Fehlberg method of seventh order (RKF7) coupled with a shooting method. In RKF7 method, thirteen evaluations are allowed for each step. For lower accuracy, this method provides the most efficient results. A step size $\Delta\eta = 0.001$ and a convergence criterion of 10^{-6} were used in the numerical computations. The far field boundary conditions in (36) were replaced by using a finite value of 10 for the similarity variable $\eta_{\max}$ as follows.

$$f'(\xi,10)=\theta(\xi,10)=\phi(\xi,10)=h(\xi,10)=0,\ \chi(\xi,10)=0 \tag{57}$$

The choice of $\eta_{\max}=10$ ensures that all numerical solutions approached the asymptotic values correctly.

5. Results and Discussion

Free convection of water-based nanofluids containing gyrotactic (torque-driven) microorganisms along a horizontal wavy surface with zero nanoparticle flux is investigated in this study. Both local similarity and non-similarity models along with boundary conditions are solved using the Runge-Kutta-Fehlberg method of seventh order (RKF7) coupled with a shooting method for both smooth and wavy surfaces. The computations are also performed when the sheet is stationary and when it is moving with uniform velocity. Mention here that for the case of stationary sheet ($\lambda = 0$) and in the case of no slip boundary conditions ($a = b = 0$), our problem reduces to that of Pradhan *et al.* [31] when $\xi = 0$ in the general mathematical developed in this article. **Table 1** presents the comparison of local similarity and non-similarity solutions for the values of reduced skin friction and local Nusselt numbers for the flow of nanofluids over smooth horizontal surface. These values are obtained for the slip flow of nanofluids over smooth horizontal stationary and moving surfaces. It is noticed that the local similarity solution *over-estimates* both skin friction and local Nusselt numbers in each case. Also, a *moving* surface reduces the skin friction and enhances the local Nusselt numbers in each case. The comparison of reduced skin friction and Nusselt numbers with existing data is presented in **Table 2** for nanofluids and regular fluids over smooth surface ($\alpha_0 = 0$) in the absence of velocity and thermal slip effects ($a = b = 0$). The computations are presented for both active and passive mass flux boundary conditions. The comparison is found to be in good agreement for the *active* boundary condition in both tables. However, for the *passive* mass flux boundary condition, the Nusselt

numbers are higher and skin friction is lower. This is due to the fact that the passive boundary condition makes the model physically more realistic than active boundary condition. It is also noticed that the reduced skin friction and Nusselt numbers increase with an increase in Prandtl number. This is attributable to the fact that the fluids with higher Prandtl number are more viscous and have relatively low thermal conductivity which increases velocity boundary layer thickness and reduces the thermal boundary layer thickness. Consequently, the shear stress and the heat transfer rate increase with Prandtl number.

Table 3 shows the computations of reduced skin friction and Nusselt numbers for both smooth and wavy surfaces and stationary and moving with uniform velocity. Both regular and water-based nanofluids are utilized in the computations. It is noticed that a moving surface (smooth or wavy) achieves higher Nusselt numbers and offers lower frictional resistance whereas a wavy surface offers both the highest frictional resistance and attains the highest Nusselt numbers. In each case, the buoyancy parameter reduces skin friction and Nusselt numbers whereas bioconvection Rayleigh number increases both skin friction and Nusselt numbers. However, Brownian motion has no significant effects on skin friction and Nusselt numbers. This is due to passive mass flux boundary condition in which both Brownian motion and thermophoresis parameters are present. Thermophoresis parameter increases skin friction and reduces Nusselt numbers.

The variation of the dimensionless velocity at the surface with wave amplitude is shown in Fig. 2(a) for a *stationary* plate and in Fig. 2(b) for a *moving* plate in the streamwise direction. It is noticed that for a smooth surface ($\alpha_0 = 0$), the dimensionless surface velocity remains constant in both cases. However, this velocity is found to be higher when the plate is moving. For a wavy surface ($\alpha_0 \neq 0$), the dimensionless velocity fluctuates between maximum and minimum values and increases with the amplitude of the wavy surface. These fluctuations increase with increasing amplitudes in the streamwise direction. This is due to the fact that the flow accelerates along the rising portions of the surface, where the slope is positive, and decelerates along the portion of the surface, where the slope is negative. The variation of the dimensionless axial pressure distribution inside the boundary layer is presented in Fig. 3(a) for a stationary surface and in Fig. 3(b) for a moving surface. The *flow is driven entirely by a pressure difference as* there is no component of buoyancy force parallel to the horizontal surface. This is due to the normal component of buoyancy and as a result the dimensionless pressure distribution is negative. Consequently, the motion of the surface does not exert any tangible influence on the boundary layer thickness. However, the motion of the surface

lowers the dimensionless pressure at the surface (Fig. 3b). It is important to note that the dimensionless pressure at the surface is *higher* and it increases with an increase in Prandtl number in both cases. In the absence of thermal slip, the surface becomes isothermal which increases the dimensionless pressure at the surface.

The effects of multiple slip (hydrodynamic and thermal) on the dimensionless temperature are depicted in Fig. 4(a) for a *stationary* surface and in Fig. 4(b) for a *moving* surface. It can be seen that the dimensionless surface temperature decreases with both velocity and thermal slips in both cases. It is well known that the velocity slip reduces the velocity at the surface whereas thermal slip reduces the dimensionless temperature at the surface for water-based nanofluids. The effects of momentum slip on the rescaled nanoparticle volume fraction are shown in Fig. 5(a) and 5(b) at a selected location for different values of Lewis number. It was assumed that the mass flux is zero at the surface. It is evident that the rescaled nanoparticle volume fraction increases with an increase in Lewis number, and as a result the rescaled nanoparticle volume fraction boundary layer thickness decreases. The velocity slip also helps in enhancing rescaled nanoparticle volume fraction within the boundary layer in both cases.

Figures 6(a) and 6(b) illustrate the variation of the rescaled density of motile microorganisms with bioconvection parameters for both stationary and moving surfaces. Unlike other boundary layers, the boundary layer for the rescaled density of motile microorganisms is found to be much thinner. In fact, bioconvection Péclet number is the ratio of the *characteristic velocity due to gyrotactic swimming* to a *characteristic velocity due to random diffusive swimming*. Since the microorganisms are heavier than water, their up-swimming creates unstable density stratification and an increase in *Rb* makes the system less stable. The bioconvection Lewis number helps in decreasing the microorganism concentration layer thickness. Physically this is because the bioconvection Lewis number rises, the *viscous diffusion rate enhances* which in turn decreases the dimensionless velocity and consequently decreases the density of the microorganisms.

The effects of scaled amplitude of the wavy surface, α_0, on the reduced skin friction are discussed in Figs. 7(a) and 7(b) for stationary and moving surfaces respectively. The effects of velocity and thermal slips are included in the computations. For a smooth surface, $\alpha_0 = 0$, the shear stress remains constant in both cases. As the amplitude of the wavy surface increases, the maximum shear stress increases. It is noted that the fluctuations in the reduced skin friction increase with the amplitude of

the wavy surface. The comparison of Figs. 7(a) and 7(b) reveals that the *reduced skin friction* is *reduced* when the surface is *moving*. The phase angle ω shows the shifting of waveform from the reference point $\xi = 0$. The maximum skin friction increases with an increase in the phase angle. The effects of multiple slips on the reduced skin friction are depicted in Figs. 8(a) and 8(b) for two different base fluids when the plate is stationary or moving. It is noticed that both velocity and thermal slips tend to reduce the skin friction in each case. It is important to note that an increase in Prandtl number enhances skin friction. This is due to the fact that Prandtl number depends upon the momentum diffusivity or kinematic viscosity of the fluid. An increase in the kinematic viscosity helps in increasing Prandtl number and consequently the skin friction increases.

In the presence of velocity and thermal slips, the reduced Nusselt numbers of water-based nanofluids are presented in Figs. 9(a) and 9(b) for stationary and moving surfaces respectively. The effects of scaled amplitude of the wavy surface, α_0, on the reduced Nusselt numbers are shown for both smooth and wavy surfaces. For a smooth surface, the reduced Nusselt numbers remain constant whereas they increase for a wavy surface. The fluctuations in the reduced Nusselt number also increase with the amplitude of the wavy surface. It is important to note that the reduced Nusselt numbers are raised when the surface is moving. The variation of reduced Nusselt number with multiple slips is shown in Figs. 10(a) and 10(b) for two different base fluids over a wavy surface. It is noticed that velocity slip and Prandtl number help in enhancing reduced Nusselt numbers while thermal slip tends to reduce the reduced Nusselt numbers in both cases. It is due to the fact that velocity slip enhances the dimensionless velocity both for the isothermal ($b = 0$) and non-isothermal ($b \neq 0$) plate. Also, due to the motion of the surface, reduced Nusselt numbers are found to be higher for the moving surface.

Figures 11(a) and 11(b) illustrate the variation of the rescaled density number of motile microorganisms with velocity slip and bioconvection parameters for both stationary and moving surfaces. This variation is shown for a nanofluid over a wavy surface at $\xi = 0.5$. In fact, bioconvection Péclet number helps in increasing the speed of the microorganisms and as a result the density number of the microorganism increases near the surface. Increasing bioconvection Lewis number assists in decreasing the microorganism concentration boundary layer thickness. This trend is induced since as the bioconvection Lewis number increases, the viscous diffusion rate increases which in turn reduces the dimensionless velocity at the surface and consequently increases the density number of the microorganisms.

6. Conclusions

A mathematical model has been developed for investigating the effect of zero mass flux boundary condition on the free convective slip flow of a water-based nanofluid with suspended gyrotactic micro-organisms along a wavy horizontal surface. The governing partial differential equations have been rendered into a set of nonlinear coupled, ordinary differential equations using suitable transformations and the resulting well-posed boundary value problem has been solved numerically using the Runge-Kutta-Fehlberg method of seventh order (RKF7) coupled with a shooting method. Local similarity and non-similarity solutions have been obtained and compared for both smooth and wavy surfaces. Numerical solutions generated have also been compared with those obtained for active mass flux boundary condition and for stationary and moving surfaces. From the present study, the main conclusions may be summarized as follows:

- A zero-mass flux boundary condition reduces the skin friction and enhances local Nusselt numbers.
- A *moving* surface reduces skin friction but conversely enhances local Nusselt numbers.
- A *wavy* surface offers higher skin friction and enhances local Nusselt numbers.
- The reduced density number of motile micro-organisms increases with bioconvection parameters and velocity slip.
- The dimensionless temperature decreases with an increase in thermal and velocity slip.
- The fluctuations in the skin friction increase with an increase in phase shift and wave amplitude along streamwise direction.

The present work has shown that nanofluids combined with bioconvection and hydrophobic slip provide a significant improvement in heat transfer rates of interest in nano-bio-fuel cell design systems.

Notation

Symbol Used

b chemotaxis constant [m]

C nanoparticle volume fraction [-]

C_w wall nanoparticle volume fraction [-]

C_∞ ambient nanoparticle volume fraction [-]

D_B Brownian diffusion coefficient [m^2s^{-1}]

D_n diffusivity of microorganisms [m^2s^{-1}]

D_T thermophoretic diffusion coefficient [m^2s^{-1}]

$f(\eta)$ dimensionless stream function [-]

g acceleration due to gravity [ms^{-2}]

$\bar{\mathbf{j}}$ vector flux of microorganism [$kgm^{-2}\ s^{-1}$]

k thermal conductivity [m^2s^{-1}]

L characteristic length [m]

Lb bioconvection Lewis number [-]

Le Lewis number [-]

m power law index [-]

n_∞ ambient density of motile microorganisms [-]

n_w density of motile microorganisms at surface [-]

$\bar{n}_n$ volume fraction of motile microorganisms [-]

Nb Brownian motion parameter [-]

$Nn_{\bar{x}}$ local density number of the motile microorganisms [-]

Nr buoyancy ratio [-]

Nt thermophoresis parameter [-]

$Nu_{\bar{x}}$ local Nusselt number [-]

Pe bioconvection Péclet number [-]

Pr Prandtl number [-]

$\bar{p}$ pressure [Pa]

Ra Rayleigh number [-]

Rb bioconvection Rayleigh number [-]

$\bar{T}$ nanofluid temperature [K]

$\bar{T}_w$ wall temperature [K]

$\bar{T}_\infty$ ambient temperature [K]

$\bar{u}, \bar{v}$ velocity components along $\bar{x}-$ and $\bar{y}-$axes [ms^{-1}]

$\tilde{\bar{u}}, \tilde{\bar{v}}$ average directional swimming velocity of microorganisms along axes [ms^{-1}]

W_c constant maximum cell swimming speed [ms^{-1}]

$\bar{x}, \bar{y}$ coordinates along and normal to the plate [m]

Greek symbols

$\bar{\alpha}$ amplitude [m]

α thermal diffusivity of fluid [m^2s^{-1}]

β coefficient of thermal expansion [K]

$\phi(\eta)$ rescaled nanoparticle volume fraction [-]

η similarity variable [-]

γ average volume of a microorganism [m^{-3}]

ν kinematic viscosity of the fluid [$m^2\ s^{-1}$]

ω phase shift [-]

ρ_f fluid density [kg m^{-3}]

ρ_p nanoparticle mass density [kg m^{-3}]

$(\rho c)_f$ heat capacity of the fluid [J $kg^{-3}K^{-1}$]

$(\rho c)_p$ heat capacity of the nanoparticle material [J kg^{-3} K^{-1}]

τ ratio between the effective heat capacity of the nanoparticle material and heat capacity of the fluid [-]

$\sigma(\eta)$ rescaled density of motile microorganisms [-]

ψ stream function [-]

$\theta(\eta)$ dimensionless temperature [-]

ξ streamwise coordinate [-]

Subscripts/superscripts

n_p nanoparticles

f fluid

w wall

∞ ambient condition

' differentiation with respect to η

References

[1] E Tombácz, D. Bica, A Hajdú, E. Illés, A. Majzik and L. Vékás, Surfactant double layer stabilized magnetic nanofluids for biomedical application, *J. Phys.: Condens. Matter* 20 (2008) 204103.

[2] T. Sharmaa, A.L. Mohana Reddy, T.S. Chandra and S. Ramaprabhu, Development of carbon nanotubes and nanofluids based microbial fuel cell, *Int. J. of Hydrogen Ener.* 33(22) (2008) 749-6754.

[3] M.M. Shaijumon, S. Ramaprabhu and N. Rajalakshmi, Platinum/ multi walled carbon nanotubes–platinum/carbon composites as electro catalysts for oxygen reduction reaction in proton exchange membrane fuel cell, *Appl.Phys.Lett*., 88**(2006)** 253105.

[4] T. Miyake, K. Haneda, S. Yoshino and M. Nishizawa, Layered biofuel cells, *Biosensors and Bioelectronics*, 40 (2013) 45–49.

[5] D. Loqué, H.V Scheller and M. Pauly, Engineering of plant cell walls for enhanced biofuel production, *Current Opinion in Plant Biology*, 25 (2015)151–161.

[6] K. Rabaey and W. Verstraete, Microbial fuel cells: novel biotechnology for energy generation, *Trends in Biotechnology*, 23 (2005) 291–298.

[7] R.A. Burton and G.B Fincher, Plant cell wall engineering: applications in biofuel production and improved human health, *Current Opinion in Biotechnology*, 26 (2014) 79–84.

[8] M.A. Hossain and D.A.S. Rees, Combined heat and mass transfer in natural convection flow from a vertical wavy surface, *Acta Mech*. 136 (1999) 133-141.

[9] J.H. Jang, W.M. Yan and H.C. Liu, Natural convection heat and mass transfer along a vertical wavy surface, *Int. J. Heat Mass Transfer*. 46 (2003) 1075-1083.

[10] A. Mahdy and S.E. Ahmed. Laminar free convection over a vertical wavy surface embedded in a porous medium saturated with a nanofluid. *Transport in Porous Media*., 91 (2012) 423–435.

[11] S.E. Ahmed and Abd El-Aziz, Effect of local thermal non-equilibrium on unsteady heat transfer by natural convection of a nanofluid over a vertical wavy surface, *Meccanica*, 48 (2013) 33–43.

[12] P.A. Lakshminarayana and P. Sibanda, Soret and Dufour effects on free convection along a vertical wavy surface in a fluid saturated Darcy porous medium, *Int. J. Heat Mass Transfer.,* 53 (2010) 3030–3034.

[13] V. Rathish Kumar and S.V.S.S.N.V.G.K Murthy, Double diffusive free convection induced by vertical wavy surface in a doubly stratified Darcy porous medium under the influence of Soret and Dufour effect, *J. Porous Media*, 15 (2012) 877–890.

[14] L.S. Yao, Natural convection along a vertical wavy surface, *ASME J. Heat Transfer*, 105 (1983) 465–468.

[15] C.Y. Cheng, Natural convection heat and mass transfer near a vertical wavy surface with constant wall temperature and concentration in a porous medium, *Int. Comm. Heat and Mass Transf.*, 27 (2000) 1143–1154.

[16] C.Y Cheng, Double diffusive natural convection along an inclined wavy surface in a porous medium, *Int. Comm. Heat Mass Transfer*, 37 (2010) 1471–1476.

[17] C.Y Cheng, Soret and Dufour effects on free convection boundary layers over an inclined wavy surface in a porous medium, *Int. Comm. Heat Mass Transfer*, 38 (2011) 1050-1055.

[18] M.S Abdallah and B. Zeghmati, Effects of the wavy surface on free convection-radiation along an inclined plate, *WASET J.*, 7 (2013) 460-466.

[19] S.J.D. D'Alessio, J.P. Pascal, H.A. Jasmine and K.A. Ogden, Film flow over heated wavy inclined surfaces, *J. Fluid Mec.*, 665 (2010) 418- 456.

[20] D. Srinivasacharya and P.V. Kumar, Effect of thermal radiation and stratification on natural convection over an inclined wavy surface in a nanofluid saturated porous medium, *Int. J. Mining, Metallurgy & Mechanical Eng.*, 3 (2015), 26-31.

[21] S. Siddiqa and M.A. Hossain, Natural convection flow over wavy horizontal surface, *Adv. Mech. Eng.*, 7 (2013) 2013. Article ID 743034.

[22] S. Siddiqa, M.A. Hossain and S.C. Saha, The effect of thermal radiation on the natural convection boundary layer flow over a wavy horizontal surface, *Int. J. Thermal Sci*., 84 (2014) 143-150.

[23] S. Siddiqa, M.A. Hossain and R.S.R. Gorla, Natural convection flow of viscous fluid over triangular wavy horizontal surface, *Computers & Fluids*, 106 (2015) 130-134.

[24] D.A.S. Rees and I. Pop, Free convection induced by a horizontal wavy surface in a porous medium, *Fluid Dyn. Res*. 14 (1994) 151-166.

[25] M. Narayana, P. Sibanda, S.S. Motsa and P.G. Siddheshwar, On double-diffusive convection and cross diffusion effects on a horizontal wavy surface in a porous medium, *Bound. Value Prob*. 88 (2012) 1-22.

[26] M.A. Hossain and I. Pop, Magnetohydrodynamic boundary layer flow and heat transfer on a continuous moving wavy surface, *Arch. Mech*. 48 (1996) 813-823.

[27] B. Tashtoush and E. Abu-Irshaid, Heat and fluid flow from a wavy surface subjected to a variable heat flux, *Acta Mechanica*, 152 (2001) 1-8.

[28] P.V.S.N. Murrhy, B.V.R Kumar and P. Singh, Natural convection heat transfer from a horizontal wavy surface in a porous enclosure. *Num. Heat Transfer, Part A: Appl.* 231 (1997) 207–221.

[29] P.B.A. Reddy, A.S. Reddy and N.B. Reddy, Magnetohydrodynamic boundary layer flow and heat transfer over a continuous moving wavy surface embedded in a porous medium, *Int. J. Appl. Math Mech.* 8 (8): 72-85, 2012.

[30] L. Pera and B. Gebhart, Natural convection boundary layer flow over horizontal and slightly inclined surfaces, *Int. J. Heat Mass Transfer*, 16 (1973) 1131–1146.

[31] K. Pradhan, S. Samanta and A. Guha, Natural convective boundary layer flow of nanofluids above an isothermal horizontal plate, *ASME J. Heat Transfer*, 136 (2014) 102501.

[32] A.J. Hillesdon, T.J Pedley and J.O Kessler, The development of concentration gradients in a suspension of chemotactic bacteria, *Bull. Math. Biol.* 57 (1995) 299–344.

[33] A.J. Hillesdon and T.J. Pedley, Bioconvection in suspensions of oxytactic bacteria: linear theory, *J. Fluid Mech*, 324 (1996) 223–259.

[34] A.V. Kuznetsov and A.A. Avramenko, Effect of small particles on the stability of bioconvection in a suspension of gyrotactic microorganisms in a layer of finite depth, *Int. Commun. Heat Mass Transf.* 31 (2004) 1–10.

[35] P. Geng and A.V. Kuznetsov, Effect of small solid particles on the development of bioconvection plumes, *Int. Commun. Heat Mass Transf.* 31 (2004) 629–638.

[36] P. Geng and A.V. Kuznetsov, Settling of bidispersed small solid particles in a dilute suspension containing gyrotactic microorganisms, Int. J. Eng. Sci. 43 (2005)992–1010.

[37] A.V. Kuznetsov and P. Geng, The interaction of bioconvection caused by gyrotactic micro-organisms and settling of small solid particles, *Int. J. Numer. Methods Heat Fluid Flow*, 15 (2005) 328–347.

[38] P. Geng and A.V. Kuznetsov, Introducing the concept of effective diffusivity to evaluate the effect of bioconvection on small solid particles, *Int. J. Transp. Phenom*., 7 (2005) 321–338.

[39] A.V. Kuznetsov, The onset of nanofluid bioconvection in a suspension containing both nanoparticles and gyrotactic microorganisms, *Int. Commun. Heat Mass Transfer*, 37 (2010) 1421–1425.

[40] A.V. Kuznetsov, Nanofluid bioconvection in water-based suspensions containing nanoparticles and oxytactic microorganisms: oscillatory instability, *Nanoscale Res. Lett*. 6 (2011) 100.

[41] A.V. Kuznetsov, Non-oscillatory and oscillatory nanofluid bio-thermal convection in a horizontal layer of finite depth, *Eur. J. Mech. – B/Fluids*, 30 (2011) 156–165.

[42] A. Aziz, W.A. Khan and I. Pop, Free convection boundary layer flow past a horizontal flat plate embedded in porous medium filled by nanofluid containing gyrotactic microorganisms, *Int. J. Therm. Sci.* 56 (2012) 48–57.

[43] J. Buongiorno, Convective transport in nanofluids, *ASME J. Heat Transfer*, 128 (2006) 240-250.

[44] A.V. Kuznetsov and D.A. Nield, The Cheng-Minkowycz problem for natural convective boundary layer flow in a porous medium saturated by a nanofluid: A revised model. *Int. J. Heat Mass Transfer*, 65 (2013) 682-685.

[45] A.V. Kuznetsov and D.A. Nield, Natural convective boundary-layer flow of a nanofluid past a vertical plate: A revised model, *Int. J. Therm. Sci.*, 77 (2014) 126-129.

[46] Z.H. Khan, W.A. Khan and I. Pop, Triple diffusive free convection along a horizontal plate in porous media saturated by a nanofluid with convective boundary condition, *Int. J. Heat Mass Transfer*, 66 (2013) 603-612.

[47] A. Shenoy, M. Sheremet and I. Pop, *Convective Flow and Heat Transfer from Wavy Surfaces: Viscous Fluids, Porous Media, and Nanofluids*, CRC Press, Florida, USA (2016).

[48] S. Sadia, M. Sulaiman, M. A. Hossain, S. Islam and Rama Subba Reddy Gorla, Gyrotactic bioconvection flow of a nanofluid past a vertical wavy surface, *Int. J. of Therm. Sci.* 108 (2016): 244-250.

[49] B. Naheed, S. Sidia and M. A. Hossain, Nanofluid bioconvection with variable thermophysical properties, *J. Mol. Liq.* 231 (2017): 325-332.

[50] M. Sheikholeslami and H. Rokni, Effect of melting heat transfer on nanofluid flow in the presence of a magnetic field using the Buongiorno Model, *Chin. J.Phys.* (2017) **In press.**

[51] F.A. Soomro, R.Ul Haq, Z.H. Khan and Q. Zang, Passive control of nanoparticle due to convective heat transfer of Prandtl fluid model at the stretching surface, *Chin. J.Phys*. (2017) **In press.**

[52] G. Karniadakis, A. Beskok and N. Aluru, *Microflows and Nanoflows: Fundamentals and Simulation*, Springer Science, New York, 2005.

[53] E.M. Sparrow and H.S. Yu, Local non-similarity thermal boundary-layer solutions, *ASME J Heat Transfer*, 93 (1978) 328-334.

[54] E.M. Sparrow, H. Quack and C.J. Boerner, Local non-similarity boundary-layer solutions, AIAA J., 8 (1970) 1936-1942.

[55] W.J. Minkowycz and E.M. Sparrow, Numerical solution scheme for local non-similarity boundary-layer analysis, *Numerical Heat Transfer, Part B: Fundamentals: An Int. J. of Computation and Methodology*, 1 (1978) 69-85.

[56] R.S.R. Gorla, A.Y. Bakier and L. Byrd, Effects of thermal dispersion and stratification on combined convection on a vertical surface embedded in a porous medium, *Trans. in Porous Med*., 25 (1996) 275–282.

[57] O. Anwar Bég, A.Y. Bakier, V.R. Prasad, J. Zueco and S.K. Ghosh, Nonsimilar, laminar, steady, electrically-conducting forced convection liquid metal boundary layer flow with induced magnetic field effects, *Int. J. Thermal Sci*., 48 (2009) 1596–1606.

[58] O. Anwar Bég, A. Y. Bakier, V.R. Prasad and S. K. Ghosh, Numerical modelling of non-similar mixed convection heat and species transfer along an inclined solar energy collector surface with cross diffusion effects, *World J. Mech.*, 1 (2011) 185-196.

Table 1: Comparison of similar and non-similar solutions for reduced skin friction and Nusselt numbers of nanofluids along smooth horizontal surface when $Lb = Pe = Le = 10, \alpha_0 = \xi = \omega = 0$ and $\Pr = 7, a = b = 0.5$.

	Local similar solution I[st] truncation				Local non-similar solution 2[nd] truncation			
	$\lambda = 0$ (stationary surface)		$\lambda = 1$ (moving surface)		$\lambda = 0$ (stationary surface)		$\lambda = 1$ (moving surface)	
Nr	Cf_r	Nu_r	Cf_r	Nu_r	Cf_r	Nu_r	Cf_r	Nu_r
	$Nb = 0.3, Nt = 0.1, Rb = 0$							
0.001	0.6117	0.3782	0.1315	0.4746	0.6109	0.3778	0.1285	0.4739
0.1	0.6114	0.3780	0.1310	0.4745	0.6105	0.3776	0.1279	0.4738
0.3	0.6106	0.3778	0.1299	0.4743	0.6098	0.3774	0.1268	0.4736
0.5	0.6098	0.3775	0.1288	0.4741	0.6090	0.3771	0.1257	0.4734
Nb	$Nr = 0.5, Nt = 0.2, Rb = 0$							
0.1	0.6074	0.3697	0.1214	0.4650	0.6055	0.3687	0.1183	0.4642
0.3	0.6152	0.3724	0.1324	0.4670	0.6133	0.3715	0.1294	0.4662
0.5	0.6167	0.3730	0.1346	0.4674	0.6148	0.3720	0.1316	0.4666
Nt	$Nr = 0.5, Nb = 0.5, Rb = 0$							
0.001	0.6047	0.3825	0.1254	0.4812	0.6038	0.3821	0.1223	0.4804
0.1	0.6106	0.3778	0.1299	0.4743	0.6098	0.3774	0.1268	0.4736
0.3	0.6167	0.3730	0.1346	0.4674	0.6227	0.3680	0.1314	0.4597
0.5	0.6360	0.3585	0.1496	0.4465	0.6357	0.3583	0.1420	0.4447
Rb	$Nr = Nb = Nt = 0.5$							
0.1	0.6564	0.3612	0.1601	0.4476	0.6556	0.3608	0.1526	0.4457
0.3	0.6950	0.3662	0.1809	0.4497	0.6941	0.3658	0.1734	0.4478
0.5	0.7309	0.3707	0.2012	0.4517	0.7301	0.3704	0.1937	0.4499

Table 2: Comparison of reduced skin friction and Nusselt numbers when $\Pr = 7, Le = 10, \alpha_0 = 0$, and $\xi = 0, \lambda = a = b = 0$ for both active and passive controls of solid volume fraction of nanoparticles.

	Pradhan *et al.* [31]		Present solution			
	Active control		Active control		Passive control	
	Cf_r	Nu_r	Cf_r	Nu_r	Cf_r	Nu_r
Nr	$Nb = 0.3, Nt = 0.1$					
0.001	0.95374	0.32878	0.95374	0.32878	0.91884	0.42066
0.1	0.93956	0.32784	0.93956	0.32784	0.91889	0.42052
0.3	0.91042	0.32591	0.91042	0.32591	0.91900	0.42023
0.5	0.88058	0.32391	0.88058	0.32391	0.91911	0.41994
Nb	$Nb = 0.4, Nt = 0.2$					
0.1	0.86002	0.35744	0.86002	0.35744	0.93076	0.41083
0.3	0.90520	0.31141	0.90520	0.31141	0.93014	0.41316
0.5	0.92979	0.26799	0.92979	0.26799	0.92998	0.41361
Nt	$Nr = 0.2, Nb = 0.3$					
0.001	0.91340	0.34076	0.91340	0.34076	0.90823	0.42699
0.1	0.92507	0.32688	0.92507	0.32688	0.91895	0.42038
0.2	0.93704	0.31362	0.93704	0.31362	0.92994	0.41373
0.5	0.97398	0.27797	0.97398	0.27797	0.96201	0.39293
Pr	$Nb = Nt = Nr = 10^{-5}$					
0.1	-	0.3114	0.8080	0.31100	0.80543	0.31036
0.72	-	0.3816	0.8580	0.38200	0.85772	0.38159
5	-	0.4224	0.9000	0.42200	0.89946	0.42175
10	-	0.4313	0.9160	0.43100	0.91278	0.42951

Table 3: Computations of reduced skin friction and Nusselt numbers for different conditions when $Lb = Pe = Le = 10, a = b = 0.5$ (Passive boundary condition).

	Smooth surface ($\alpha_0 = 0$)				Wavy surface ($\alpha_0 = \xi = \omega = 0.5$)			
	Stationary surface ($\lambda = 0$)		Moving surface ($\lambda = 1$)		Stationary surface ($\lambda = 0$)		Moving surface ($\lambda = 1$)	
	Cf_r	Nu_r	Cf_r	Nu_r	Cf_r	Nu_r	Cf_r	Nu_r
Nr	$Nb = 0.3, Nt = 0.1, \Pr = 7, Le = 10$							
0	0.66330	0.38479	0.15848	0.47714	1.10128	0.44044	0.54356	0.51658
0.1	0.66292	0.38467	0.15796	0.47705	1.10143	0.44036	0.54327	0.51650
0.3	0.66216	0.38441	0.15690	0.47686	1.09035	0.43651	0.54269	0.51633
0.5	0.66140	0.38415	0.15584	0.47668	1.09065	0.43634	0.54210	0.51617
Nb	$Nr = 0.4, Nt = 0.2, Pr = 7, Le = 10$							
0.1	0.81653	0.40024	0.24739	0.47878	0.68231	0.42290	0.73519	0.52456
0.3	0.68775	0.38176	0.16998	0.47047	1.14534	0.43800	0.57583	0.51143
0.5	0.67087	0.37954	0.16221	0.46974	1.10007	0.43049	0.55490	0.50986
Nt	$Nb = 0.3, Nr = 0.2, \Pr = 7, Le = 10$							
0.001	0.63884	0.38637	0.14222	0.48243	1.06288	0.44223	0.51197	0.52097
0.1	0.66146	0.38401	0.15564	0.47652	1.08442	0.43510	0.54179	0.51618
0.3	0.68926	0.38226	0.17209	0.47084	1.14486	0.43833	0.57699	0.51175
0.5	0.79523	0.37984	0.24155	0.45608	1.30111	0.43553	0.71030	0.50078
Le	Pr=7,Nr=Nb=Nt=0.5							
5	0.73011	0.37652	0.19741	0.45841	1.21451	0.43242	0.63167	0.50110
10	0.73010	0.37035	0.19998	0.45140	1.21145	0.42570	0.63189	0.49386
100	0.71165	0.35170	0.19317	0.43348	1.18174	0.40586	0.61058	0.47424
Pr	Le=10,Nr=Nb=Nt=10^{-5}							
3	0.68253	0.38563	0.08712	0.46665	1.11985	0.43983	0.48142	0.50794
5	0.69970	0.39332	0.14659	0.47982	1.15244	0.44911	0.55483	0.52120
10	0.71909	0.40118	0.21268	0.49340	0.50499	0.37798	0.63697	0.53481
15	0.72804	0.40455	0.24333	0.49934	0.50528	0.37833	0.67555	0.54078

FIGURES

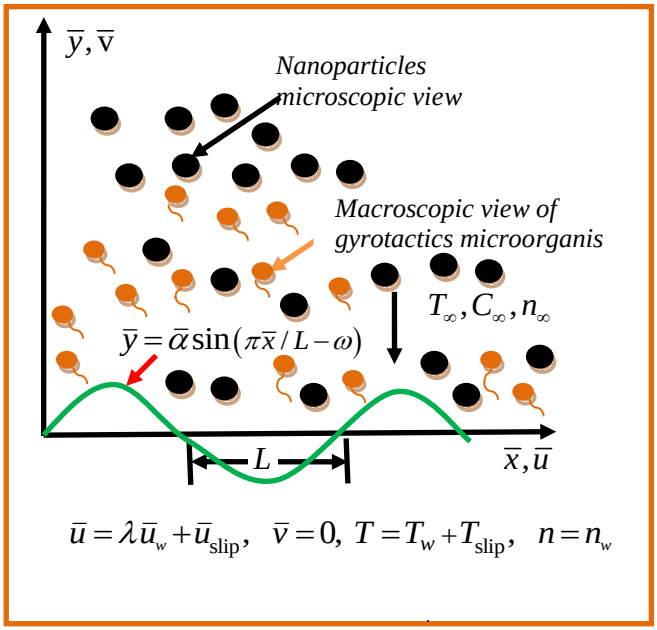

Fig. 1: Biological flow diagram of wavy surface (microbial fuel cell wall)

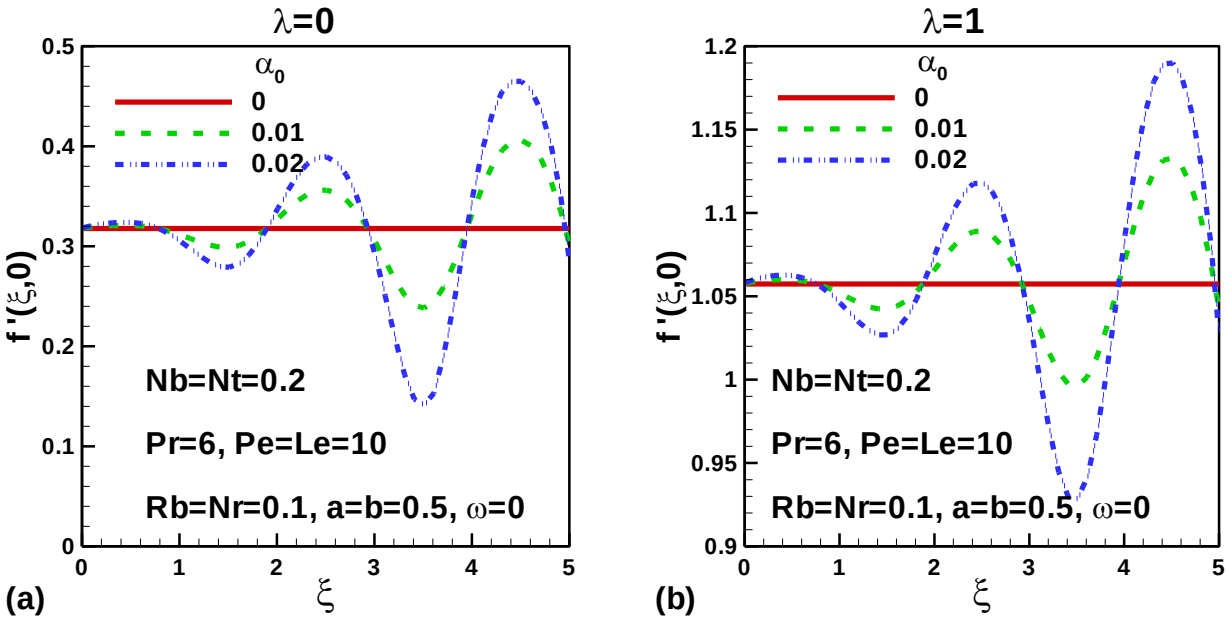

Fig.2: Variation of dimensionless velocity with wave amplitude along streamwise direction when (a) plate is stationary and (b) plate is moving.

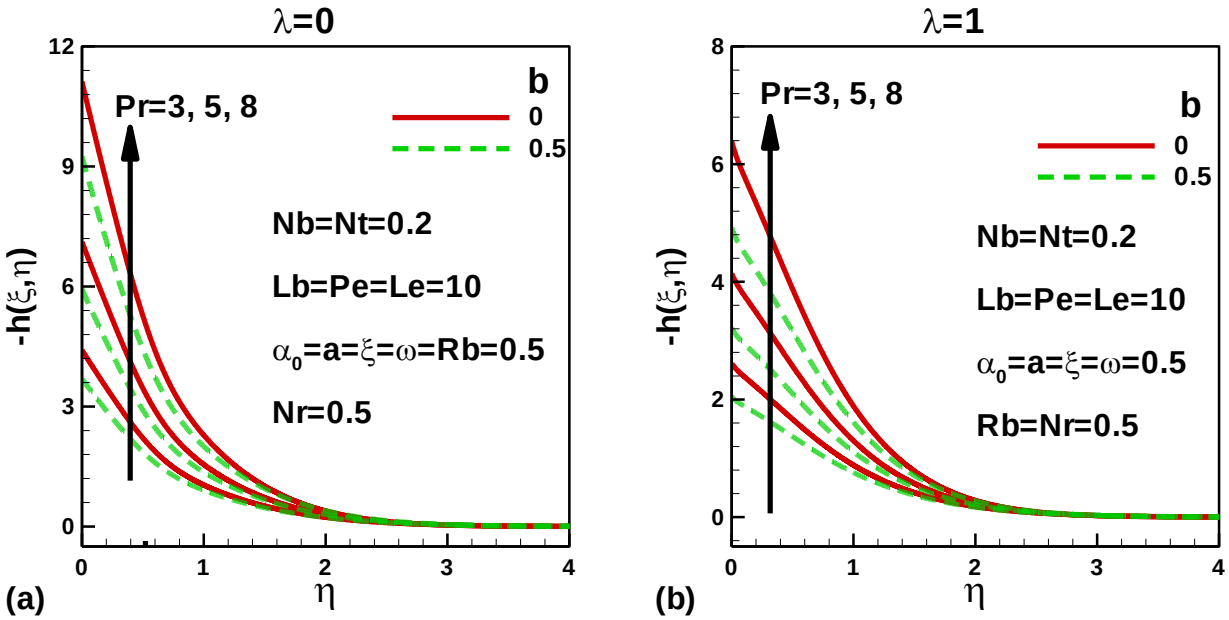

Fig. 3: Variation of dimensionless axial pressure distribution with thermal slip and Prandtl number when (a) plate is stationary and (b) plate is moving.

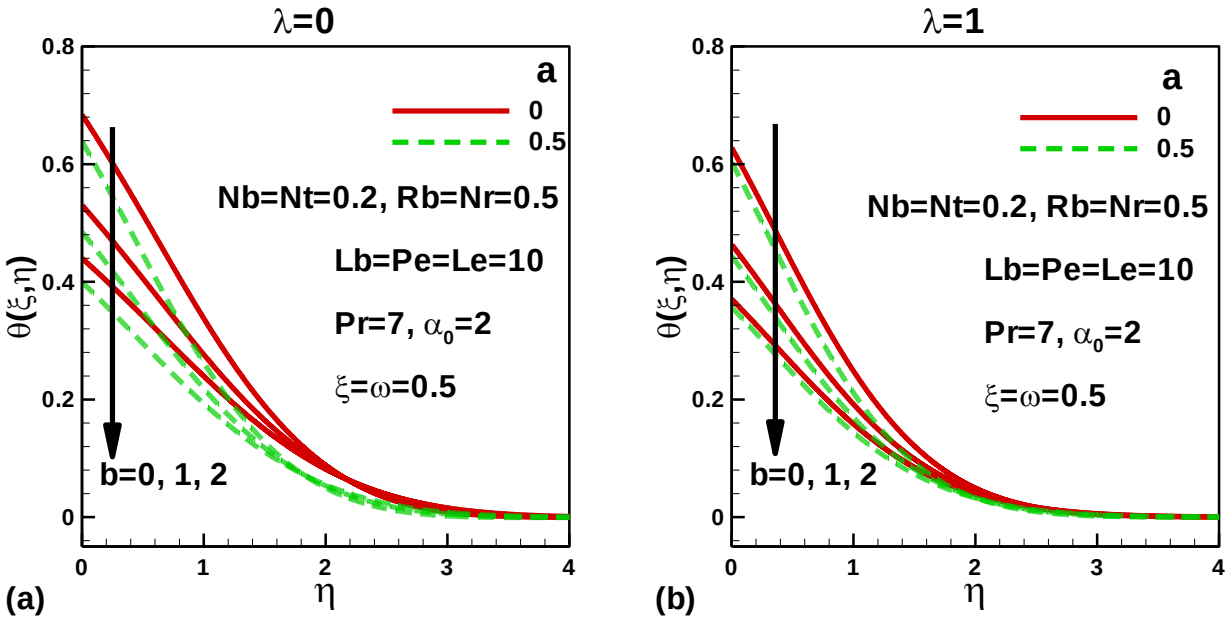

Fig. 4: Variation of dimensionless temperature with thermal and velocity slip when (a) plate is stationary and (b) plate is moving.

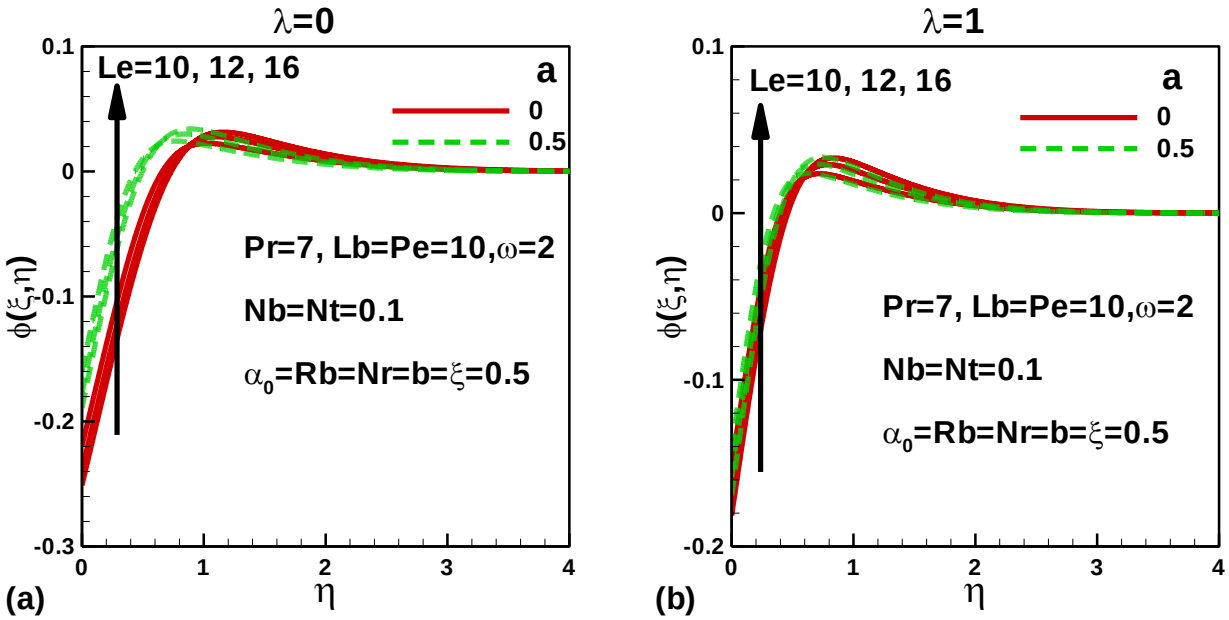

Fig. 5: Variation of dimensionless rescaled nanoparticle volume fraction with Lewis number and velocity slip when (a) plate is stationary and (b) plate is moving.

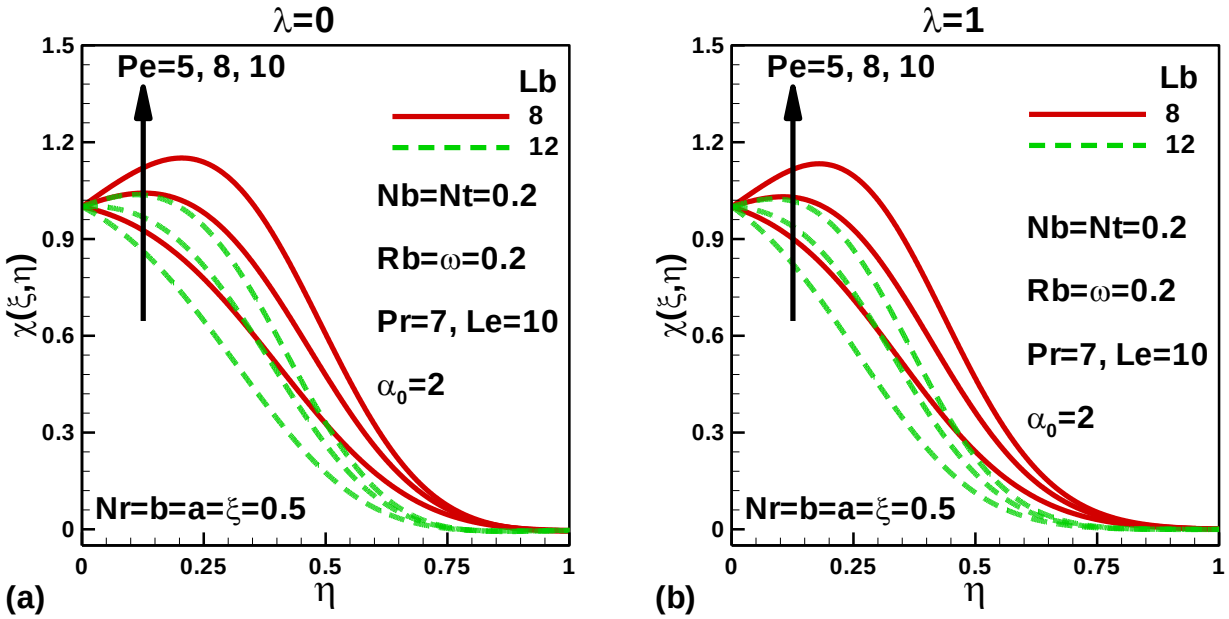

Fig. 6: Variation of rescaled density of motile microorganisms with bioconvection parameters when (a) plate is stationary and (b) plate is moving.

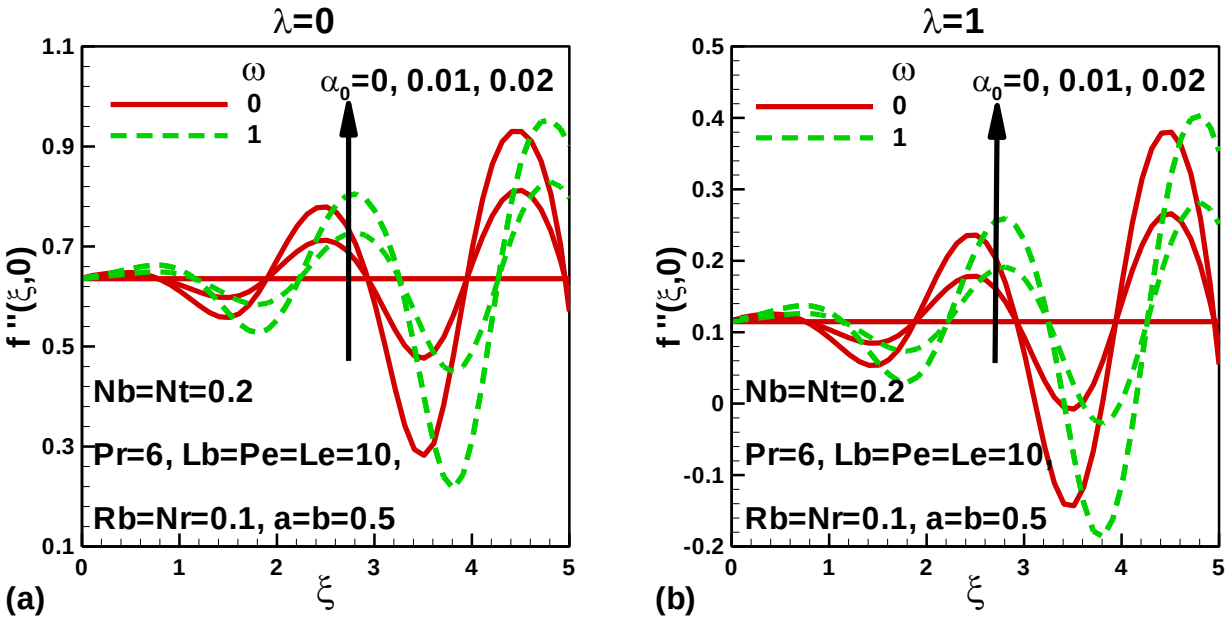

Fig. 7: Variation of skin friction with phase shift and wave amplitude along streamwise direction when (a) plate is stationary and (b) plate is moving.

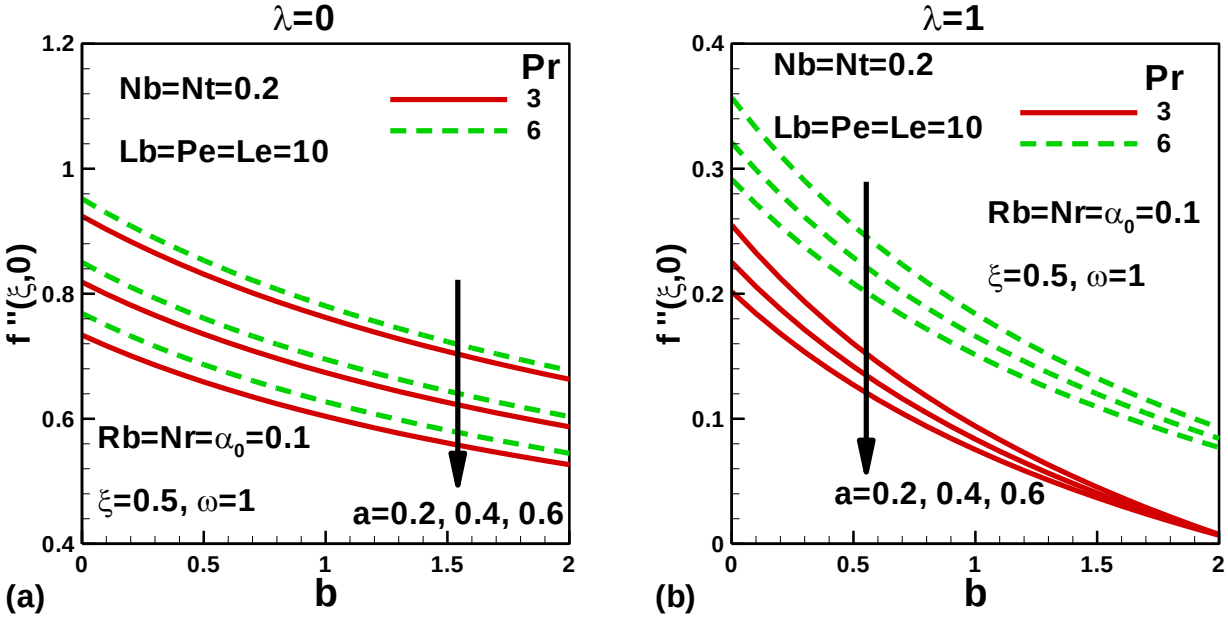

Fig. 8: Variation of reduced skin friction with velocity and thermal slips for two different base fluids when (a) plate is stationary and (b) plate is moving.

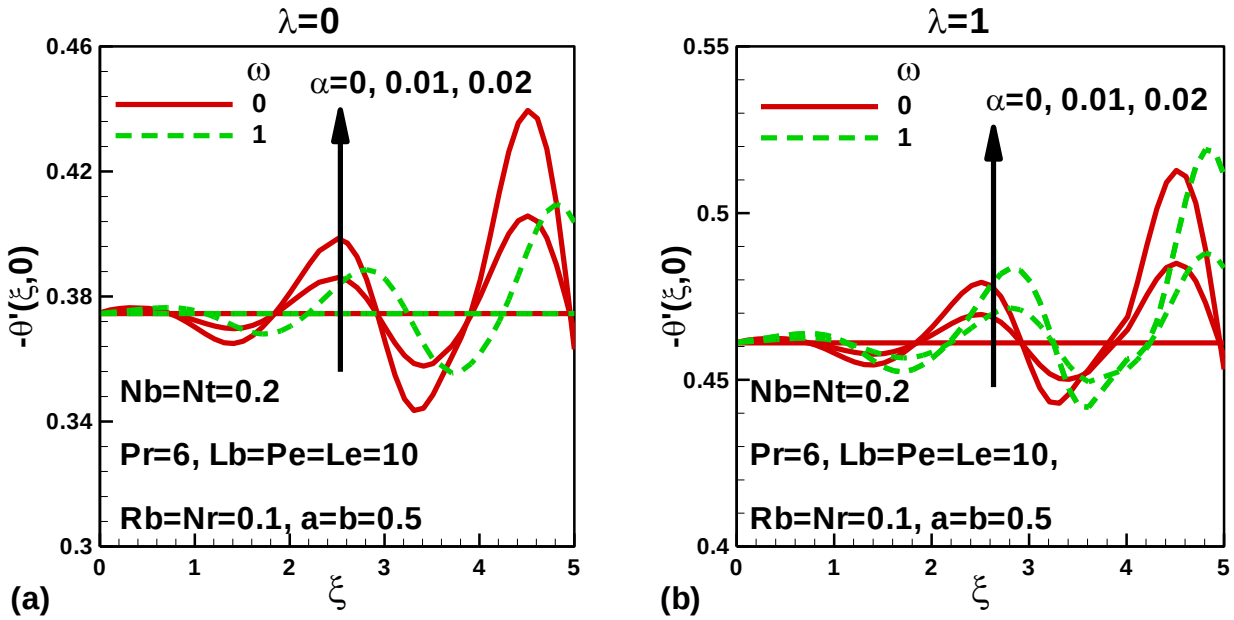

Fig. 9: Variation of reduced Nusselt number with phase shift and wave amplitude along streamwise direction when (a) plate is stationary and (b) plate is moving.

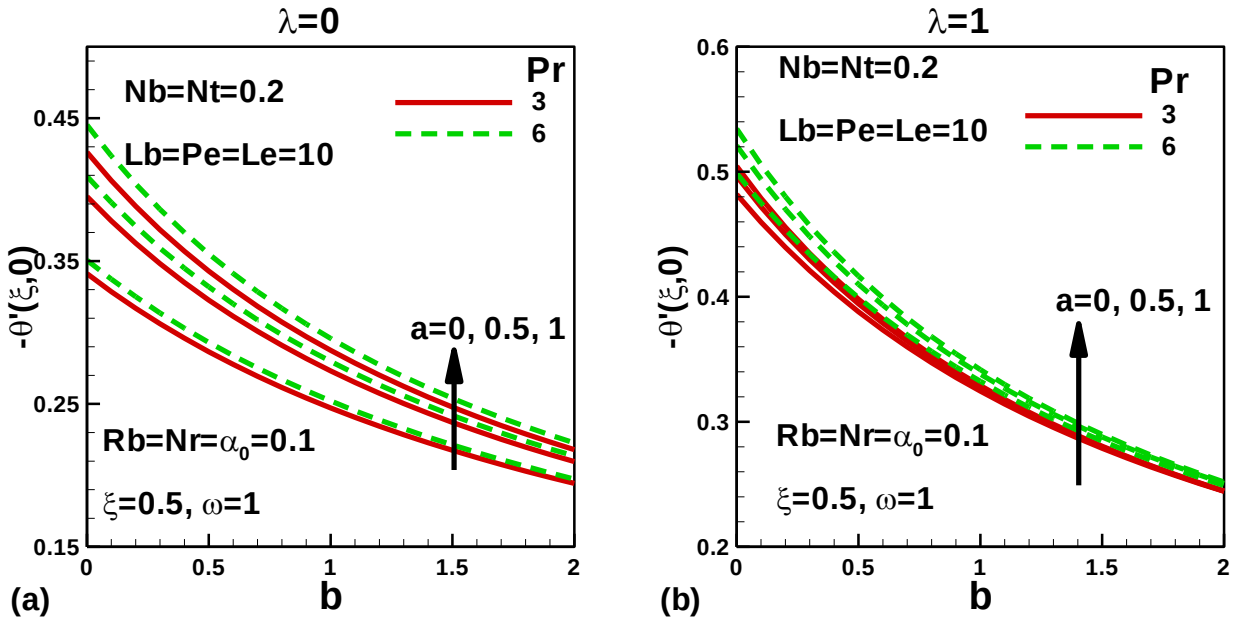

Fig. 10: Variation of reduced Nusselt numbers with velocity and thermal slips for two different base fluids when (a) plate is stationary and (b) plate is moving.

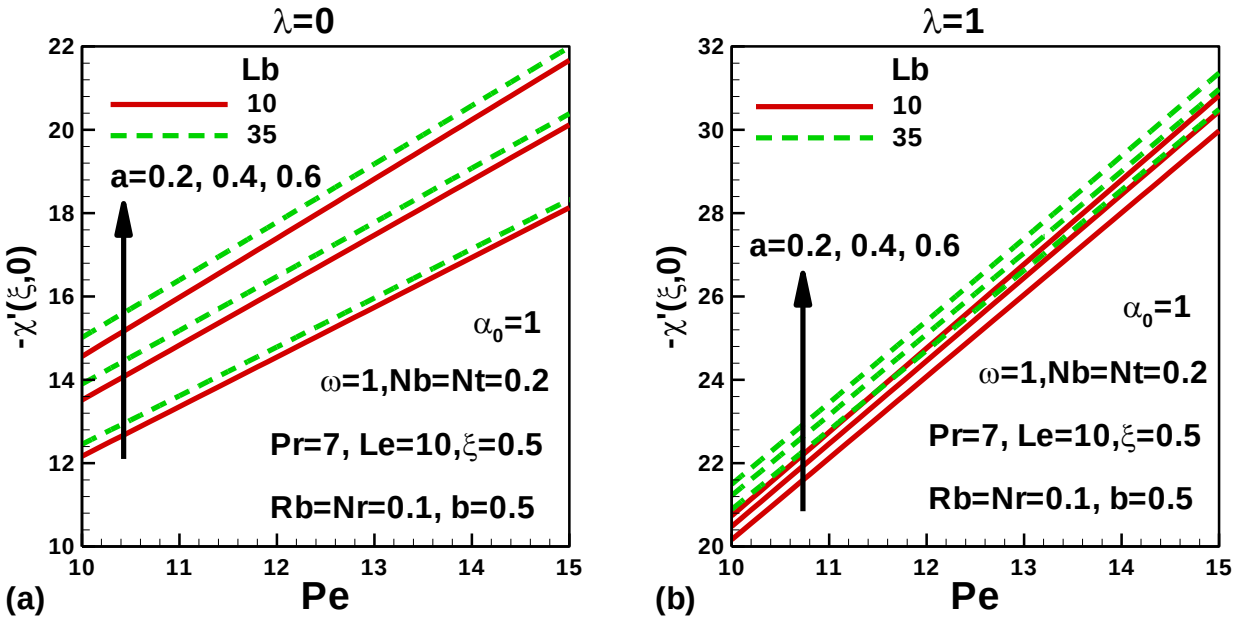

Fig. 11: Variation of reduced density number of motile microorganisms with bioconvection parameters and velocity slip when (a) plate is stationary and (b) plate is moving.